Sohar University Journal of Engineering and Information Technology Innovations (SUJEITI), ISSN: 3078-7513
Volume 2, Issue 2, pp 20-32, June 2026, DOI: 10.69983/SUJEITI/2242
Received: 24/05/2026 Revised: 29/055/2026 Accepted: 09/06/2026

# Energy and Exergy evaluation of Photovoltaic Thermal (PVT) system cooled by nanofluid and Spiral Flow Absorber

**Miqdam T Chaichan[1,2], Hussein A Kazem[2,3*]**

[1]Energy and Renewable Energies Technology Center, University of Technology, P. O. Box: 10065, Baghdad, Iraq, miqdam.t.chaichan@uotechnology.edu.iq
[2]Faculty of Engineering, University of Sohar, P. O. Box: 44, Sohar, PCI 311, Oman, h.kazem@su.edu.om
[3]UNESCO RCQE Chair in Emerging Renewable & Sustainable Energy Technologies, Sohar University, PO Box 44, Sohar, PCI 311, Oman
*Corresponding author email: h.kazem@su.edu.om

## Abstract

The performance of a nanofluid-cooled PVT collector can be represented by its electrical and thermal efficiencies. The sum of the two efficiencies, known as the overall PVT system efficiency, is used to evaluate the overall system performance. A PVT system powered by a Multi-Wall Carbon Nanotube (MWCNT) nanofluid was constructed and investigated in Baghdad-Iraq climates. Experimental results demonstrated that both efficiencies increase with increasing mass flow rate, and consequently, the overall efficiency (PVT efficiency) increases. The nanofluid-cooled PVT system equipped with a spiral-flow heat exchanger achieved overall PVT efficiencies ranging from 59% to 70%, with electrical efficiencies ranging from 12.8% to 13.5% and thermal efficiencies ranging from 46.2% to 56.5%. These efficiencies were achieved at mass flow rates ranging from 0.011 kg/s to 0.033 kg/s and a solar irradiance of from 250 to 1000 W/m². Recently, exergy analysis has been applied to evaluate PVT collector performance more comprehensively. In the study, the analyses show that the PVT exergy efficiency is between 22% and 40% with thermal exergy of 572 to 118 W and electrical exergy of 59 to 67 W.

***Keywords**:* college teaching; student evaluations of teaching; online administration; response rate; assessment

## 1. Introduction

The photovoltaic (PV) systems have become an ever-growing concern of significance to the global environment since they play a critical role in energy production and climate change control. The frequency with which fossil fuels are being burnt and the increased environmental concerns have advanced the transition to using renewable sources of power, and one of the most available and clean sources of energy is solar energy. The PV technology has also made solar power more accessible across the world due to improvement in efficiency and cost reduction. Moreover, the intensive use of the PV system has been triggered by government policies and incentives that encourage the use of clean energy. The fact that they can produce electricity in isolated locations that are not connected to the grid also boosts energy security and helps to develop economically. With this need to have clean, reliable, and affordable

energy, the photglobalystems prove to be a prospective solution to the global energy demand, as well as the reduction of carbon emissions and helping in achieving a sustainable future (Jassim et al., 2025).

In recent years, there has been tremendous improvement in the PV unit cooling technologies in an effort to enhance the efficiency and durability of photovoltaic systems. Active, passive, and hybrid cooling methods are becoming more popular in the effort to minimize thermal buildup, which is a significant cause of efficiency degradation (Ali et al., 2025). Advanced cooling techniques comprise heat pipe-based cooling, heat sinks, nanofluid-aided cooling, phase change materials (PCM), thermoelectric, and multifunctional coating (Appalasamy at al., 2025; Alinia et al., 2025). There are systems with temperature decreases of more than 40°C and efficiency gains of over 15%. These cooling systems are used to maintain optimal conditions of PV panels under high irradiance and temperature settings of the sun (Kazem et al., 2021).

PVT systems are also becoming significant in increasing numbers because they are able not only to achieve electricity but also to capture the thermal energy, thereby making the most out of the overall solar energy. The benefits of having PVT systems are that they are energy efficient since they generate electrical and hot water or heat, which helps in improving energy savings, decreasing fossil fuel reliance, and decreasing greenhouse gas emission. Such a combination of applications allows making PVT systems a promising solution of sustainable energy management in high-demand areas (Gad et al., 2025).

Nanoparticles and nanofluids have emerged as highly important in improving the heat transfer processes through exceptional thermal properties. Nanoparticles are dispersed in base fluids to create nanofluids that are more effective in thermal conductivity and heat transfer efficiency and are approximately 30 times better than traditional fluids and consist of nanoparticles (usually metals or metal oxides, such as MgO, $TiO_2$, and ZnO). The dispersibility and stability of nanoparticles should be uniform to enhance performance to the maximum. The key nanoparticles are metallic, oxide, carbon-based, and ceramic, which have a different effect on the fluid viscosity, density, and heat transfer properties. Nanofluids are promising for future effects in compact and efficient thermal systems in electronics, solar energy, and industrial heat exchangers, which can result in superior energy efficiency and reduced system size. Their increasing significance is associated with the increased need for better cooling of more advanced technologies, which can revolutionize thermal systems in different spheres (Hanif et al., 2022; Mamat 2019; Zareei et al., 2025; Rahman et al., 2024).

The thermal conductivity of multi-wall carbon nanotube (MWCNT) nanoparticles is truly phenomenal, with values of 2000-6000 $W/m^2$ K, and this is much more than the conventional metallic or oxide nanoparticles. MWCNTs are also known to increase thermal conductivity, the coefficient of convective heat transfer, and boiling heat transferred when suspended in base fluids to form nanofluids, which has great potential in enhancing the cooling [10]. Experimental results indicate an increase in the heat transfer coefficient of 11.5% to a greater percentage of more than 30 percent with the concentration of MWCNT. They have a high aspect ratio and a distinctive form, which helps enhance the superior heat transport mechanism compared to the nanoparticles that have a spherical shape (Apmann et al., 2022). Typical examples are different functionalized MWCNTs to enhance dispersion stability of fluids. These nanofluids promise to be useful in thermal control in electronics, power sectors, and solar thermal equipment, allowing more efficient, compact, and sustainable technologies to be developed. The applications of MWCNT nanofluids in the future are likely to transform the energy systems through improved thermal control and efficiency in various industrial and renewable energy applications (Progar et al., 2024; Rashid et al., 2023; Chaichan et al., 2023).

The experimental analysis of the exergy produced in a PVT system cooled by a nanofluid provides a more insightful analysis compared to the traditional energy analysis. Whereas energy analysis measures the total heat and electricity produced, exergy analysis measures the quality or usability of the energy produced by the system by considering the irreversibilities and entropy generated in the system. This enables one to know the point and the nature of the inefficiencies and losses and make more specific improvements. In the case of nanofluid-cooled PVT systems, exergy analysis demonstrates the efficiency of better transfer of heat to eliminate the thermodynamic losses and hence optimize the overall performance of the system. It also measures the efficiency of the system in converting solar energy into valuable electrical and thermal output. Finally, the use of exergy analysis in addition to energy analysis will make it easier to design more efficient and sustainable systems of PVTs with improved economic and environmental value, particularly in situations where more sophisticated cooling methods are employed, such as the nanofluids (Al-Aridhee et al., 2023; Rukman et al., 2019).

Most studies on the performance of PVT systems have focused solely on electrical and thermal energy analysis. Most researchers avoid exergy analysis due to its complexity. This study will analyze the energy and exergy of a PVT system using nanofluid cooling composed of water (the base fluid) and MWCNT-water nanofluid. The aim of this study is to analyze the energy and exergy for a PVT system equipped with a spiral flow absorber and cooled by

MWCNT nanofluid. The productivity of such a system will be compared to a water-cooled system. The study will focus on the effects of mass flow rate on energy and exergy efficiencies.

## 2. Experimental Setup

### 2.1. Study Area

Iraq, and specifically Baghdad, has severe environmental and climatic problems, and severe weather experienced during summer is one of them. Iraq is a very susceptible country to climatic change with increasing temperatures and water deficiency and desertification in most of their agricultural lands. Summers are very hot and dry with cold and dry winters in Baghdad (Muslih et al., 2024). The summers in Baghdad are hot and dry, and the temperatures may go beyond 44.4°C and may even hit 51.7°C. The city receives little to no rainfall between June and September, worsening the severity of drought. Combined with urban heat islands, bad air quality, and loss of green areas through rapid urbanization, this extreme heat is worsened by the fact that more than half of the parks in Baghdad have been overwhelmed by urban sprawl (Abdulkareem et al., 2021).

The air in Baghdad is usually perilous, and the pollution level is significantly higher than the permissible one, which, in turn, aggravates the situation in summer. These are poor environmental conditions that pose danger to the health of the people, the sustainability of agricultural activities, and the general life quality. The predictions of climate change indicate a further rise in temperature and environmental decline, which means that the mitigation strategies should be implemented promptly to fight these severe summer conditions and their broader consequences (Aljuhaishi et al., 2025). Therefore, Baghdad can be discussed as the bright example of the hot desert climate characterized by the extreme environmental pressure, hot and humid summer, high level of dryness, and new pollution issues (Hamed et al., 2025; AbdulKareem et al., 2025).

### 2.2. System Description

A spiral flow design was chosen for this study as the heat exchanger. This design was constructed from spiral-shaped copper cooling tubes, leaving space only for the junction box. This design proved to be more efficient at transferring heat compared to other designs, as shown in Reference (Fudoli et al., 2013). Thermal silicone oil was used before soldering the tubes to the back of the photovoltaic panel to secure the copper tubes, and a layer of glass wool was used as a solar insulator at the back of the collector. The photovoltaic modules used in the study were of the polycrystalline silicon type with a power of 100 watts. The overall dimensions of the tested photovoltaic cell module were 1014 × 669 mm, equivalent to a total area of 0.678 m². The collector area was defined as the effective thermally connected area with the copper spiral cooling tubes, excluding the junction box area and other ineffective margins, where the junction box area was 0.0080 m². From this, it is clear that the PVT system active area fraction is about 98.82% of the PV module area.

The tests were conducted indoor using a MINI-EESTC solar thermal unit, Italy made. A photovoltaic panel is placed on top of the top plate. Silicone oil was used to coat the top and bottom surfaces of the panel to prevent the formation of any air gaps, which may affect heat transfer between the PV panel and the collector. The photovoltaic cell is exposed to directed irradiance from fifteen incandescent lamps, providing a variable luminous intensity ranging from 0 to 1500 W/m². The solar simulator has a control panel that adjust the radiation intensity.

**Table 1:** Specifications of typical photovoltaic module

| **Electrical performance under Standard Test Conditions (S.T.C)** | **Specification** |
|---|---|
| **Model** | SPM100P-TS-N |
| **Rated power (Pmax)** | 100 W |
| **Open-circuit voltage (Voc)** | 22.8 V |
| **Short-circuit current (Isc)** | 5.76 A |
| **Voltage at Pmax (Vmp)** | 18.6 V |
| **Current at Pmax (Imp)** | 5.38 A |
| **PV module electrical efficiency** | 14.8% |
| **Dimensions** | 1014 x 669 x 35 mm |

| | | |
|---|---|---|
| **Weight** | 9 kg | |

This simulator includes a liquid circulation pump, allowing the system to operate in either forced or natural convection modes. The

Experimental setup shown in Figure 1 consisted of five temperature sensors, one of them being the room temperature sensor. As not all radiant energy is collected by the collector plate and is converted to light and not all electrical energy is converted to light, three curtains are used to enclose the collector on three sides, and the base of the liquid tank blocks the fourth side. Four thermocouples were also placed to measure the changes in temperature in the system with the liquid pump. Figure 1 shows the experimental setup (PVT system tested by MINI-EESTC solar simulator unit).

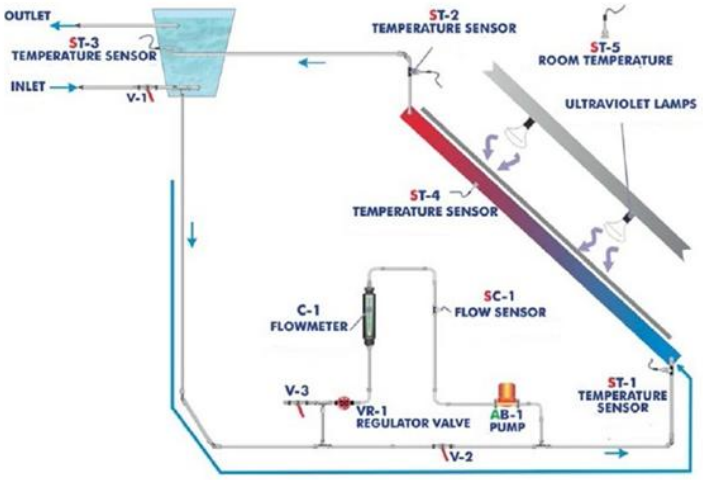


**Figure 1:** A schematic diagram of the indoor solar simulator parts.

### 2.3. Nanofluid Preparation Process

Using the methods used in reference (Chaichan et al., 2023), nanofluids using water and MWCNTs were prepared in order to be as stable as possible. Table 2 gives the nanomaterial properties that are critical in bringing information about how they will behave after mixing. To dry the nanoparticles, an oven with a temperature of 200°C was used, and they were allowed 15 minutes. Nanoparticles are dispersed in deionized water by 1% proportion of weight. It was hard to obtain stable nanofluids at the desired concentrations without the surfactants, and, therefore, approximately 0.1 mL of Cetyl-Trimethyl Ammonium Bromide (CTAB) was incorporated. The analytical balance (EJ6I0-E) was used to weigh nanoparticles precisely. They were carefully put into a 12-liter ultrasonic bath (TELSONIC ULTRASONICS CT-I2) and sonicated throughout 3.5 hours to disrupt agglomerates and create a stable, homogenous suspension. The concentration of MWCNT in the final nanofluid was 1.0% in water.

**Table 2:** Specifications and physical properties of the nanoparticles used in this study

| Particle | Density ($\rho_p$) ($kg/m^3$) | Thermal conductivity ($k_p$) (W/m °C) | Purity | Size ($d_p$) (nm) | Color | Supplier |
|---|---|---|---|---|---|---|
| **MWCNT** | 2,400 | 480.0 | 96.00% | 50-150 | Black | Nanografi (Ankara TURKEY) |

By doing this, the temperature and nanofluid stability are ensured and are essential in ensuring that an experiment is accurate and reproducible.

The evaluation of the thermophysical properties of the prepared nanofluid were as follows:

1. Density was measured by weighing 250 mL samples for each nanoparticle concentration and dividing by volume. Literature indicates the base liquid primarily influences density, while nanoparticle size and shape have minor effects.

2. Viscosity was measured using a Brookfield programmable viscometer (LVDV-III) connected to a PC for data logging.

3. Thermal conductivity was assessed with a HOT DESK Tps 500 meter (KIJTALEY, Sweden), employing an isotropic method accurate to over 97.5%, with measurement durations from 2.5 to 2560 seconds.

4. Specific heat was measured using a thermal calorimeter (ESD-201).

All the above measurements were repeated three times to ensure repeatability, and average values were taken to minimize uncertainty from random errors.

This rigorous methodology guarantees precise characterization of the nanofluid's physical and thermal behavior for reliable experimental results and analysis.

### 2.4. Uncertainty Analysis

Calibration of all measurement instruments was also done to evaluate the error produced during the experiment in this study. The difference between the true value and the measured one of a quantity is referred to as error. Determining the magnitude of such an error permit calculating the uncertainty of each measurement; that is, the level of confidence in the outcome. The term "uncertainty" is presented in accordance with the definition of reference, which explains it as a parameter that indicates the dispersion of any of the possible values measured relative to an optimal estimate. To measure the reliability of experimental data and take into consideration systematic and random errors involved in measurement procedures, it is crucial to perform proper uncertainty assessment. This would make reported results indicate some realistic limits on accuracy and precision, which would support the validity of conclusions made based on the experiments. The following equation is used to compute the uncertainty in the results.:

$$e_R = \sqrt{\left(\frac{\partial R}{\partial V_1} e_1\right)^2 + \left(\frac{\partial R}{\partial V_2} e_2\right)^2 + \cdots + \left(\frac{\partial R}{\partial V_n} e_n\right)^2} \quad (1)$$

Where: $e_R$ : Uncertainty in the results; R: a given function of the independent variables V1, V2, …, Vn or R=R(V1, V2, …, Vn). ei : uncertainty interval in the nth variable; $\frac{\partial R}{\partial V_1}$ - The sensitivity of a measured result for a single variable. The resulting value of the experiment's uncertainty was less than 3%, which indicates a high accuracy was achieved in these tests. Table 3 shows the measurement devices, measured parameters, and associated experimental uncertainties

**Table 3:** Measurement devices, measured parameters, and associated experimental uncertainties

| Equipment | Parameter | Experimental uncertainty |
|---|---|---|
| **Density meter** | Nanofluid density | ±0.78% |
| **Viscosity meter** | Viscosity | ±1.01% |
| **KD2 Pro device** | Thermal Conductivity | ±0.68% |
| **Precision Scale** | Nanoparticles' weight | ±0.22 |
| **Solar radiation intensity meter** | Irradiance | ±0.89% |
| **Temperature sensors** | Temperature (collector's inlet, outlet, and ambient) | ±1.12 °C |
| **Flow measurement device** | Coolants' flow rate (kg/s) | ±0.34 |

### 2.5. Experimental procedures

The first experiment involved the preparation of nanofluids by combining MWCNT nanoparticles and deionized water in a given volumetric ratio using the mixing protocol that had been described earlier. Afterward, the physical characteristics of the obtained nanosuspensions, such as density, viscosity, thermal conductivity, and stability, were completely described. A solar simulation system was used to undertake the experimental tests. At first, water was used as the cooling fluid, and they were tested at 0.011, 0.022, and 0.033 kg/s flow rates; afterwards, the results were compared with the results that were achieved with the MWCNT nanofluid at the same flow rates. This comparative analysis was aimed at the impact of each fluid on the work of this system.

Since the external solar intensity varies over time and the environment, the indoor solar simulator was coded to reflect such variations. The experiments began with a light intensity of 250 W/m² at 7:00 AM, increasing by 75 W/m² every half hour. The intensity was gradually increased to 1000 W/m² at 12:00 PM and maintained at this level for the next two hours. Starting at 2:00 PM, the irradiance was reduced by 75 W/m² every half hour. This method was used

because it closely approximates what occurs under actual outdoor conditions. To allow a fair assessment, two PVT systems were employed, one of which was cooled with water and the other with the nanofluid. The official aim was to establish the most effective fluid flow rate in order to attain the maximum performance of the PVT system. This systematic work would be used to guarantee a thorough comparison of the fluid cooling efficiency in different patterns of solar irradiation.

### 2.6. Energy Analysis

The system performance was evaluated using the following equations:

The system's thermal efficiency is:

OBJ (2)

Where, $A_c$ is the collector area and $I_s$ is the solar intensity.

The PV electrical power is:

$$P = I \times V \quad (3)$$

Where, V is the voltage and I is the current.

The useful collected heat (W)

$$Q_u = \dot{m} C_p (T_o - T_i) \quad (4)$$

Where, $\dot{m}$ is the mass flow rate, Cp is the specific heat (J/kg K) and To and Ti are outlet and inlet fluid temperatures.

The electrical efficiency $\eta_e$ is:

$$\eta_e = \frac{P}{I_s \times A_c} \quad (5)$$

Where, Ac is the PV panel area.

The total efficiency ($\eta_t$) = the thermal efficiency + the electrical efficiency

$$\eta_t = \eta_{th} + \eta_e = \frac{Q_u + P}{I_s \times A_c} \quad (6)$$

Where, Ac is the total area of the PV panel and collector.

### 2.7. Exergy Analysis

Exergy is used to measure the maximum useful work that a given system can do when at equilibrium and provides a more subtle measure of the quality of energy because it is known that various forms of energy do not work in the same manner in different situations. Exergy considers the environmental parameters such as temperature and pressure to determine the usability of energy, unlike energy that has restrictions in its usage according to the situation at hand. The exergy efficiency analysis in PVT systems shows the irreversibility and losses. Although the enhancement of electricity generation causes a slight decrease in exergy, the impacts of the level of the solar radiation and the size of the collectors have stronger negative impacts. Quality of energy depends on the temperature variation between the system and its environment, and so energy and exergy are required to completely characterize the condition of a system. The energy production is only related to the system state, and exergy production also relates to the environmental conditions. The second law of thermodynamics restricts transformation of energy to exergy as it is important to reduce reflections in order to achieve the best possible work output. This is an important principle of maximizing the efficiency of PVT systems. The analysis framework of exergy is described in the following equations. The next equation was used to determine the exergy analysis.

Electrical exergy (W) (Nourpour et al., 2023):

$$E_{X_{Electrical}} = \eta_e I = \zeta_e I \quad (7)$$

Thermal exergy (W):

$$E_{X_{Thermal}} = Q_u \left[1 - \frac{T_a + 273}{T_{fo} + 273}\right] \quad (8)$$

Electrical exergy efficiency (%) (Alsarraf et al., 2023):

$$\eta_{E_{X\,Elect}} = \frac{E_{X_{Electrical}}}{E_{X_{in}}} \quad (9)$$

Thermal exergy efficiency (%) (Li et al., 2020; Chaichan et al., 2024):

$$\eta_{E_{X\,Thermal}} = \frac{E_{X_{Thermal}}}{E_{X_{in}}} \quad (10)$$

## 3. Results and Discussions

### 3.1. Thermophysical properties of the tested nanofluid

The key thermophysical properties of pure water and a prepared nanofluid with 1% of MWCNTs are compared for the range of temperatures 25–65°C, as shown in Table 3. It demonstrates the effect of a small volume fraction of high-conductivity nanoparticles on the change of density, viscosity, thermal conductivity, specific heat, and colloidal stability of the base fluid.

The density of the material increases slightly as the number of nanoparticles is increased at all temperatures. At 25°C, water has a density of 997 kg/m³, whereas the 1% MWCNT nanofluid reaches 1005 kg/m³; by 65°C, the values are 980.5 and 989 kg/m³, respectively. This slight rise is due to the higher solid density of carbon nanotubes and is representative of low-concentration nanofluids. The viscosity change is more apparent in the case of the nanofluid; it decreases from 1.34 mPa s at 25°C to 0.66 mPa s at 65°C, whereas the viscosity of water decreases from 0.890 to 0.44 mPa s. This implies that for the same flow conditions the energy consumption or the pressure drop of the pumping system to be used for the nanofluid will be greater than the energy consumption or pressure drop of the corresponding pumping system for water, and this trade-off should be taken into account in the design of thermal systems.

Although studies suggest that nanofluids improve heat transfer performance—often by increasing effective thermal conductivity or disrupting thermal boundary layers—this benefit must be weighed against any potential increase in hydraulic loss. Specifically, the addition of nanoparticles alters the viscosity of the base fluid, particularly at higher particle concentrations. Nanoparticles can also increase wall friction due to changes in velocity gradients near the wall, or, in some cases, surface roughness effects if particles settle or accumulate. Therefore, simply reporting an improvement in heat transfer without specifying the corresponding increase in pumping capacity and pressure drop is insufficient. To account for these factors, the pressure drop and the required pumping capacity increase were neglected; however, these two factors are critical when operating on a large-scale system.

The main motivation for using MWCNTs is the enhancement in thermal conductivity. Table 3 shows that the conductivity of water is slightly higher at higher temperatures, from 0.60 to 0.65 W/m K, while that of the nanofluid is higher, from 0.73 to 0.79 W/m K. Hence, at 25°C the nanofluid shows conductivity enhancement of approximately 22%, and even at 65°C, the enhancement remains to be around 21–22%, which can greatly enhance convective heat-transfer coefficients in heat exchangers or cooling channels. The specific heat is also almost unchanged, approximately 4.18 kJ/kg K for water and 4.15 kJ/kg K for the nanofluid, showing that the amount of energy that can be stored per unit mass is only slightly decreased by the addition of the nanotubes.

**Table 4:** Thermophysical properties of the prepared nanofluid

| **Temp. (°C)** | **Density (kg/m3)** | | **Viscosity (mPa-s)** | | **Thermal Conductivity (Wm-1K-1)** | | **Specific heat (kJ/kg K)** | | **Stability [Zeta potential (\|ζ\|) (mV)]** | |
|---|---|---|---|---|---|---|---|---|---|---|
| | Water | Nano-MWCNT (1%) | Water | Nano-MWCNT (1%) | Water | Nano-MWCNT (1%) | Water | Nano-MWCNT (1%) | Water | Nano-MWCNT (1%) |
| **25** | 997 | 1005 | 0.890 | 1.34 | 0.6 | 0.73 | 4.18 | 4.15 | - | 53 |
| **35** | 994 | 1002 | 0.719 | 1.08 | 0.62 | 0.75 | 4.18 | 4.15 | - | 54 |
| **45** | 990 | 998 | 0.596 | 0.89 | 0.63 | 0.76 | 4.18 | 4.15 | - | 56 |
| **55** | 985.7 | 994 | 0.5 | 0.75 | 0.64 | 0.78 | 4.18 | 4.15 | - | 57 |
| **65** | 980.5 | 989 | 0.44 | 0.66 | 0.65 | 0.79 | 4.18 | 4.15 | - | 59 |

Lastly, the zeta potential is given as a measure of the colloidal stability of a nanofluid. The values are between 53 and 59 mV in magnitude in the temperatures studied, and there is no entry for the zeta potential of water because there are no dispersed particles. Zeta potentials in the range of approximately 30 mV or higher above the reported value of the magnitude indicate good electrostatic stabilization, and the 1% MWCNT suspension can be considered stable against aggregation and sedimentation under the tested conditions, necessary to have consistent properties in practical applications.

### 3.2. Changes in PV module temperature

Figure 2 shows the evolution of the surface temperature of PV with time when under various cooling fluids and flow rates, where the simulated solar irradiance increases slowly at a rate of between 250 W/m² and 1000 W/m². The surface temperature of PV increases with time (between 8:00 AM and 4:00 PM). The highest temperature is reached around 1pm-2pm, with the solar irradiance staying at 1000 W/m2. Predictably, the rising solar irradiance causes the rise of PV surface temperature.

The results of the different mass flow rates of coolants are quantified in Table 5 in terms of decrease in PV module surface temperature compared to the uncooled reference (PV only).

The PV (67–68°C) is used as a baseline without cooling. A very small quantity of water cooling (0.011 kg/s) results in a small drop to approximately 64–65°C, suggesting that convective heat removal is limited at low water flow. Further increasing the water flow to 0.022 kg/s and 0.033 kg/s slightly reduces the surface temperature to ~ 60–61°C and ~ 58–59°C, respectively, with the corresponding surface cooling rates of ~ 7 and ~ 8°C, respectively, showing the improvement of forced convection and proximity to single-phase cooling behavior.

**Table 5:** PV panels' surface temperatures drop for the tested systems

| **Fluid flow rate (kg/s)** | **PV surface temperature** | **Temperature drop compared to no cooling** |
|---|---|---|
| **PV only** | ~ (67-68) | 0 |
| **Water (0.011)** | ~ (64-65) | ~ 2-3 |
| **Water (0.022)** | ~ (60-61) | ~ 7 |
| **Water (0.033)** | ~ (58-59) | ~ 8 |
| **Nanofluid (0.011)** | ~ (57-58) | ~10 |
| **Nanofluid (0.022)** | ~ (50-52) | ~16-18 |
| **Nanofluid (0.033)** | ~ (45-47) | ~20 |

The cooling effect of nanofluid is always higher than that of water for the same cooling rates when the two are used at the same flow rates, as a result of higher effective thermal conductivity and better convective heat transfer coefficients. At 0.011 kg/s, nanofluid lowers the PV temperature to 57–58 °C (~ 10°C drop), while 0.022 kg/s brings it down to 50–52 °C (~ 16–18°C drop). The optimum performance is obtained at 0.033 kg/s nanofluid, which excels at producing a surface temperature of about 45-47°C with an overall reduction of ~ 20°C compared to the uncooled panel, which is beneficial for the electrical efficiency as well as the thermal recovery of PVT operation.

The outcome indicates that a higher flow rate of cooling water lowers the amount of surface temperature of the PV panels considerably, thereby probably enhancing the effectiveness of the system in heat management with increasing solar energy intensity.

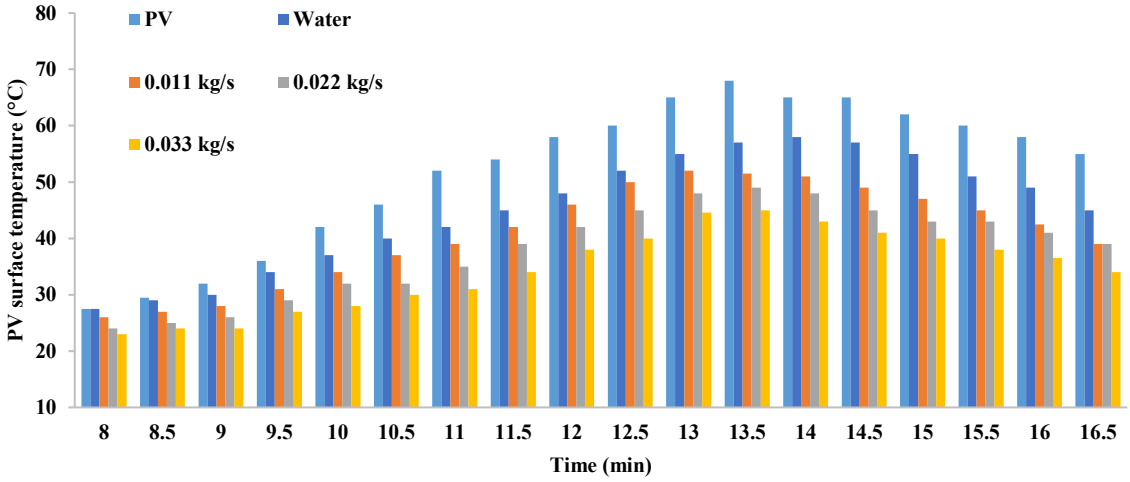


**Figure 2:** The effect of daytime on PV surface temperature for the tested systems.

### 3.3. Energy efficiency

In Figure 3, the energy performance of all four tested configurations is depicted in relation to the amount of solar power received by the system, commonly referred to as incident solar irradiance. The thermal performance of all four configurations will generally increase as there is more solar energy incident upon the PV/T collectors, from about 250 W/m² up to approximately 1,000 W/m² (which is an approximate range of solar energy incident upon typical PV/T systems). The nanofluids—the nanofluid-based PV/T system exhibits the most significant increase in thermal performance, demonstrating a rapid increase in thermal performance as solar radiation increases, peaking during the early afternoon (approximately 1:30) before tapering off slightly at the extreme irradiance values due to being close to the practical limits of heat transfer coefficients and increased convective and radiative losses from the absorber. Conversely, the water-cooled PVT system exhibits a more gradual upward trend with its thermal performance until it reaches quasi-steady-state conditions for both the absorber and coolant at elevated irradiance levels. PV electrical efficiency for a stand-alone PV system change very little with changing irradiance levels; in fact, it decreases slightly with increasing irradiance levels because the temperature of the PV cells will typically increase as the rate of irradiance increases while their temperature tends to be maintained through the active cooling that occurs in the PVT configurations, resulting in equivalent or slightly improved electrical efficiencies for the PV/T configurations.

The highest thermal efficiency of a photovoltaic under concentration (PVT) system utilizing a nanofluid was roughly 50%; when at the same irradiation level, a water-cooled version of the same system has an efficiency of only ~23%. This highlights the superior ability of the nanofluid to extract heat from the PVT system. The PVT system at the highest thermal efficiency had a mass flow rate of ~0.033 kg/sec (not shown). It is also evident that if the mass flow rate is reduced, for example, to 0.011-0.022 kg/sec, the convection heat transfer coefficient will decrease, and less thermal energy can be displaced from the PV absorber by water during operation, thereby reducing thermal energy available from the PV systems. The nanofluid's effective thermal conductivity and superior convective behavior in the absorber channels create a much larger temperature difference between the PV absorber and the coolant, thus displacing more thermal energy and therefore lower the operating temperature of the PV cells. Additionally, nanofluid-cooled PVT systems maintain PV layers at optimum temperatures during periods of high irradiance, which produce small but detectable improvements in electrical efficiency and significantly greater improvements in thermal efficiency compared to their conventional water counterparts. Overall, evidence suggests that the performance of PVT systems is optimized by maximizing the intensity of solar radiation and that nanofluid cooling provides the most effective means of providing thermal management of PVT systems, resulting in maximum combined thermal benefit for minimal changes in electrical efficiency.

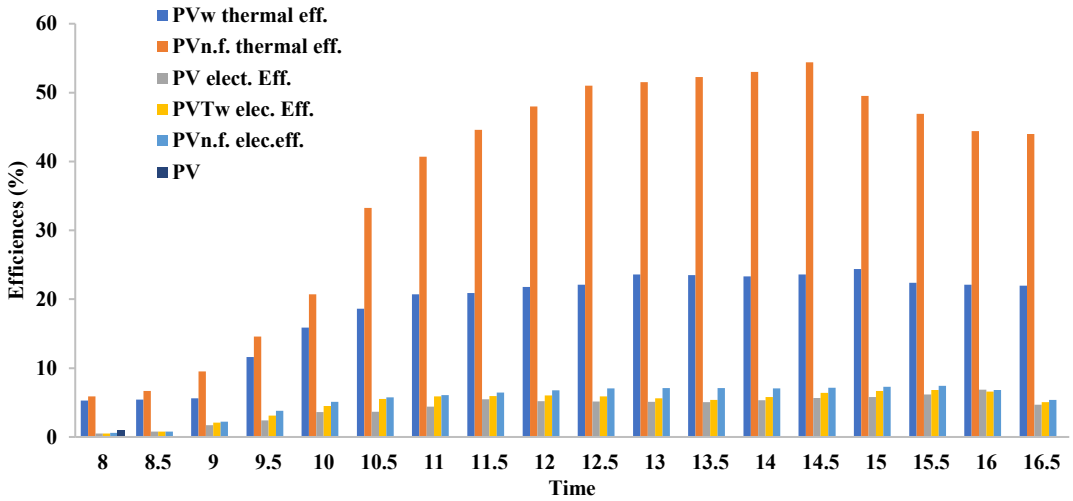


**Figure 3:** The effect of daytime on the tested systems' energy efficiencies.

The water-cooled system shows fair improvement, but less than nanofluid. Electrical efficiency benefits moderately from improved cooling, but thermal gains dominate the system performance enhancement in PVT systems under varying solar irradiation conditions. This confirms the advantages of using MWCNT nanofluid in PVT systems for optimized cooling and maximum performance at varied solar intensities.

### 3.4. Exergy Efficiency

The relationship between solar irradiance and the associated PVT exergy efficiency is shown in figure 4. Individual factors that affect the second law performance of the system include (1) incident exergy, (2) the type of coolant flowing through the heat exchangers, and (3) the flow rate of the coolant. As solar irradiance increases between around midday at approximately 1000 W/m², the exergy efficiencies of all configurations exhibit the same general pattern, increasing until they reach their maximum value (peak) just after solar irradiance is at its highest, before stabilizing at about that same maximum value or decreasing slightly thereafter. The above-described patterns in exergy performance can be attributed to two opposing forces acting on the PV solar energy system: First, as solar irradiance increases, the amount of solar exergy being delivered to the collector aperture increases. Conversely, as the PV solar energy system operates at a higher temperature due to higher solar incidence, the PV cells lose exergy more quickly due to higher levels of irreversibility occurring in both the PV cells and the associated solar liquid heat exchanger. As a result of these facts, to achieve optimum values of exergy efficiency, high levels of solar irradiance must occur in conjunction with effective thermal management practices that will limit exergy losses due to elevated temperatures of the PV and the working fluid.

At all levels of irradiance, nanofluid-cooled PVT systems have consistently greater exergy efficiencies compared to their thermally and electrically equivalent water-cooled counterparts with the same mass flow rate. As a result, not only does the nanofluid absorb greater quantities of thermal energy from the incoming solar energy, but it also converts a greater percentage of this energy into usable electrical and thermal energy (exergy) as a result of being able to generate less entropy in the collector during this conversion process. Similar to the case of MWCNT and hybrid-nanofluid studies, the gain in exergy efficiency can be several percentage points (that is, approximately 6 to 7 percentage points or greater) as compared to that produced by water for matched test conditions, which is significant in terms of the second law of thermodynamics. The increase in mass flow rate will improve the exergy efficiency of the system up to some optimal value due to the enhancement of convective heat transfer and the reduction of the temperature of both the PV and the cooling fluid, but beyond that, there will be little to no increased temperature reduction (and therefore exergy destruction) due to the further increase in pumping power used up to that point.

From a thermodynamic perspective, the use of nanofluids for cooling PV cells provides superior thermal performance than using only water. When nanofluids are used to control the PV cell temperature, this results in reducing entropy generation in both the electrical energy produced and the thermal system. Although the electrical exergy efficiency improves slightly due to temperature control, the majority of the total exergy efficiency of cells can be accounted for by using better heat recovery methods and lowering the exergy losses associated with the absorber and heat removal system. This is evidenced by the significantly more pronounced peaks in observed exergy

efficiencies of the nanofluids shown in Figure 4 as compared to the flatter peaks associated with water cooling, particularly for the region with moderate-to-high levels of irradiance, where thermal management is most important for good operation. Therefore, utilizing nanofluid-based cooling technology provides for maximum use of available solar exergy and minimum irreversibility of components, assuming that the intensity of solar radiation and flow provides an optimum configuration of performance together.

**Figure 4:** The effect of daytime on the tested systems' exergy efficiencies.

## 4. Conclusion

This paper designed and experimentally analyzed a photovoltaic thermal system with a spiral flow absorber and multi-walled carbon nanotube-water nanofluid cooling and was experimented on at simulated solar conditions to replicate the hot climate of Baghdad. The experiment involved the preparation of a nanofluid, determination of thermophysical properties (density, viscosity, thermal conductivity, specific heat), experiments with an indoor solar simulator at different mass flow rates (0.011-0.033 kg/s), and energy/exergy analyses to determine the electrical, thermal, and overall efficiency of nanofluid cooling versus water cooling.

The suggested solution would increase PVT performance through the increased heat transfer of MWCNT nanofluids, which is 50 percent higher compared to 23% of water, and lower PV surface temperatures by 20°C under optimized flow rates and exergy efficiencies through minimized irreversibilities. The total efficiencies were up to 59-70%, with exergy of 22-40%, indicating potential cogeneration of sustainable energy in arid areas.

Such features as compact design, high thermal control through spiral flow and nanofluids, dual-electrical/thermal output, and extreme climates are advantages. Disadvantages include the complexity of preparation of nanofluid (sonication, surfactants), increased viscosity/pumping energy, long-term stability, and increased prices of MWCNTs. Future directions ought to focus on the hybrid nanofluids (e.g., MWCNT-$Al_2O_3$), long-term outdoor testing, economic modeling, phase change material integration to have passive cooling, and AI-controlled flow to take it to the next level.

## Acknowledgment

The authors would like to acknowledge University of Technology for supporting this research.

**Author contribution:** All authors have contributed, read, and agreed to the published version of the manuscript results.

**Conflict of interest:** The authors declare no conflict of interest.

**Nomenclature**

| | |
|---|---|
| $A_c$ | Collector's area $(m^2)$ |
| $C_p$ | Specific heat in $(kJkg^{-1}K^{-1})$ |
| $E_{X_{Electrical}}$ | Electrical exergy (W) |
| $E_{X_{Thermal}}$ | Thermal exergy (W) |
| $E_{water}$ | Energy retained in the water (W) |
| F | Tubes' number |
| I | Current (A) |
| L | Tube's length (m) |
| $M$ | Mass (kg) |
| P | Power (W) |
| Q | Heat transfer (W) |
| $S_T$ | Total solar radiation received daily $(kJm^{-2})$ |
| $T_o$ | Outer temperature (°C) |
| $T_{in}$ | indoor temperature (°C) |
| $T_0$ | Surroundings absolute temperature (in K). |
| V | Voltage (V) |

| | |
|---|---|
| $\eta$ | Efficiency (%) |
| $\eta_{Ex\,Thermal}$ | Thermal exergy efficiency (%) |
| $\varepsilon$ | Exergy efficiency (%) |

## References


[1]. Jassim, L., Mnati, H. M., Abd Ali, F. A. M., & Majdi, H. S. (2025). Photovoltaic-driven cooling systems: advances, challenges, and future directions. Al-Rafidain Journal of Engineering Sciences, 191-209. https://doi.org/10.61268/yws21607

[2]. Ali, A. O., Elgohr, A. T., El-Mahdy, M. H., Zohir, H. M., Emam, A. Z., Mostafa, M. G., ... & Elhadidy, M. S. (2025). Advancements in photovoltaic technology: A comprehensive review of recent advances and future prospects. Energy Conversion and Management: X, 26, 100952. https://doi.org/10.1016/j.ecmx.2025.100952

[3]. Appalasamy, K., Mamat, R., & Kumarasamy, S. (2025). Smart thermal management of photovoltaic systems: Innovative strategies. AIMS Energy, 13(2), 309-353. https://doi.org/10.3934/energy.2025013

[4]. Alinia, A. M., & Sheikholeslami, M. (2025). Development of a new solar system integrating photovoltaic and thermoelectric modules with paraffin-based nanomaterials. Scientific Reports, 15(1), 1336. https://doi.org/10.1038/s41598-025-85161-5

[5]. Kazem, H. A., Al-Waeli, A. H., Chaichan, M. T., & Sopian, K. (2021). Numerical and experimental evaluation of nanofluids based photovoltaic/thermal systems in Oman: Using silicone-carbide nanoparticles with water-ethylene glycol mixture. Case Studies in Thermal Engineering, 26, 101009. https://doi.org/10.1016/j.csite.2021.101009

[6]. Gad, R., & Hassan, H. (2025). Enhancing the performance of low-concentrated solar panel/thermal system via an indirect passive cooling system of phase change material with water. Applied Thermal Engineering, 128125. https://doi.org/10.1016/j.applthermaleng.2025.128125

[7]. Hanif, H., & Shafie, S. (2022). Interaction of multi-walled carbon nanotubes in mineral oil based Maxwell nanofluid. Scientific Reports, 12(1), 4712. https://doi.org/10.1038/s41598-022-07958-y

[8]. Mamat, H. (2019). Effect of Multi-Walled Carbon Nanotubes Concentrations on Heat Transfer in Nanofluid. Malaysian Journal of Microscopy, 15(1).

[9]. Zareei, J., Guerrero, J. W. G., Formanova, S., Prasad, K. D. V., & Widatalla, S. T. H. (2025). Effects of carbon nanotube concentration on heat transfer characteristics in turbulent mixtures. International Journal of Thermofluids, 28, 101326. https://doi.org/10.1016/j.ijft.2025.101326

[10]. Rahman, M. A., Hasnain, S. M., Pandey, S., Tapalova, A., Akylbekov, N., & Zairov, R. (2024). Review on nanofluids: preparation, properties, stability, and thermal performance augmentation in heat transfer applications. ACS omega, 9(30), 32328-32349. https://doi.org/10.1021/acsomega.4c03279

[11]. Apmann, K., Fulmer, R., Scherer, B., Good, S., Wohld, J., & Vafaei, S. (2022). Nanofluid heat transfer: enhancement of the heat transfer coefficient inside microchannels. Nanomaterials, 12(4), 615. doi: 10.3390/nano12040615. PMID: 35214944; PMCID: PMC8880719.

[12]. Porgar, S., Huminic, G., Huminic, A., Najibolashrafi, R., & Salehfekr, S. (2024). Application of nanofluids in heat exchangers-A state-of-the-art review. International Journal of Thermofluids, 24, 100945. https://doi.org/10.1016/j.ijft.2024.100945

[13]. Rashid, U., Lu, D., & Iqbal, Q. (2023). Nanoparticles impacts on natural convection nanofluid flow and heat transfer inside a square cavity with fixed a circular obstacle. Case Studies in Thermal Engineering, 44, 102829. https://doi.org/10.1016/j.csite.2023.102829

[14]. Chaichan, M. T., Kazem, H. A., Al-Ghezi, M. K., Al-Waeli, A. H., Ali, A. J., Sopian, K., ... & Al-Amiery, A. A. (2023). Effect of different preparation parameters on the stability and thermal conductivity of MWCNT-based nanofluid used for photovoltaic/thermal cooling. Sustainability, 15(9), 7642. https://doi.org/10.3390/su15097642

[15]. Al-Aridhee, S. T. A., & Moghiman, M. (2023). Yearly energy, exergy, and environmental (3E) analyses of a photovoltaic thermal module and solar thermal collector in series. Al-Khwarizmi Engineering Journal, 19(1), 36-56. https://doi.org/10.22153/kej.2023.01.001

[16]. Rukman, N. S. B., Fudholi, A., Taslim, I., Indrianti, M. A., Manyoe, I. N., Lestari, U., & Sopian, K. (2019). Energy and exergy efficiency of water-based photovoltaic thermal (PVT) systems: an overview. International Journal of Power Electronics and Drive Systems, 10(2), 987-994. http://doi.org/10.11591/ijpeds.v9.i3.pp1367-1373

[17]. Muslih, K.D. and Abbas, A.M., 2024. Climate of Iraq. In The Geography of Iraq (pp. 19-47). Cham: Springer Nature Switzerland.

[18]. Abdulkareem, I. H., & Nemah, H. A. (2021). Variation of weather elements during different seasons in Iraq. Journal of Engineering Science and Technology, 16(6), 5000-5012.

[19]. Aljuhaishi, S., Al-Timimi, Y., & Wahab, B. (2025). Spatio-temporal Variation of Weather Systems and their Seasonal Variability in Iraq.

[20]. Hamed, Z. Q., & Kadhum, S. A. (2025). Trends in Air Pollution in the Middle and South of Iraq: As Climate Change Evidence in the Region. International Journal of Environmental Sciences, 11(3s), 165-179.

[21]. AbdulKareem, N. W., Al-Lami, A. M., & Al Maliki, A. (2025). Assessment of stable isotopes characteristics of rainwater in Baghdad city, Iraq. Iraqi Journal of Science, 3803-3817. https://doi.org/10.24996/ijs.2025.66.9.24

[22]. Fudholi, A. H. M. A. D., Ibrahim, A., Othman, M. Y., Ruslan, M. H., Kazem, H. A., Zaharim, A., & Sopian, K. (2013, October). Energy and exergy analyses on water based photovoltaic thermal (PVT) collector with spiral flow absorber. In 2nd International Conference on Energy Systems, Environment, Antalya, Turkey (pp. 70-74).

[23]. Nourpour, M., Khoshgoftar Manesh, M. H., Pirozfar, A., & Delpisheh, M. (2023). Exergy, exergoeconomic, exergoenvironmental, emergy-based assessment and advanced exergy-based analysis of an integrated solar combined cycle power plant. Energy & Environment, 34(2), 379-406.
[24]. Alsarraf, J., Alnaqi, A. A., & Al-Rashed, A. A. (2023). Simulation of two-phase hybrid nanofluid flow in a flat plate solar collector equipped with spiral absorber tube under the influence of magnetic field: Hydraulic-thermal, energy, and exergy analysis. Journal of Magnetism and Magnetic Materials, 585, 171120.
[25]. Li, M., Zhong, D., Ma, T., Kazemian, A., & Gu, W. (2020). Photovoltaic thermal module and solar thermal collector connected in series: Energy and exergy analysis. Energy Conversion and Management, 206, 112479.
[26]. Chaichan, M. T., Kazem, H. A., Abd, H. S., Al-Waeli, A. H., & Sopain, K. (2024). Evaluation of photovoltaic thermal system performance with different nanoparticle sizes via energy, exergy, and irreversibility analysis. Case Studies in Thermal Engineering, 64, 105499.